Solitary Fibrous Tumor of the Uterus Presenting With Lung Metastases: A Case Report

Article *in* International journal of gynecological pathology: official journal of the International Society of Gynecological Pathologists · June 2015

DOI: 10.1097/PGP.0000000000000197

International Journal of Gynecological Pathology
00:1–5, Lippincott Williams & Wilkins, Baltimore

Case Report

Solitary Fibrous Tumor of the Uterus Presenting With Lung Metastases: A Case Report

Kyle C. Strickland, M.D., Ph.D., Marisa R. Nucci, M.D., Katharine M. Esselen, M.D., M.B.A., Michael G. Muto, M.D., Sameer Chopra, M.D., Ph.D., Suzanne George, M.D., and Brooke E. Howitt, M.D.

Summary: We describe the case of an 81-yr-old woman who presented with bilateral pulmonary nodules in the setting of a large uterine mass, concerning for a gynecologic malignancy such as leiomyosarcoma. However, fine-needle aspiration of a lung nodule revealed a spindle cell neoplasm consistent with solitary fibrous tumor (SFT), a rare mesenchymal neoplasm characterized by a patternless architecture of spindle cells and branching ectatic vessels. Total abdominal hysterectomy demonstrated a primary SFT of the uterus. Both the lung lesion and uterine mass were positive for STAT6, a sensitive and specific biomarker for SFT. SFT infrequently metastasizes and only rarely occurs in the uterus. These tumors are considered to have uncertain malignant potential, and the diagnosis of "malignant" SFT requires the presence of >4 mitoses per 10 high-power fields. The uterine SFT we report did not meet this criterion for malignancy, emphasizing that this entity can behave aggressively even without increased mitoses or atypical histology. To our knowledge, this is the first reported case of a uterine SFT with metastasis to the lung. We discuss the differential diagnosis for the finding of multiple pulmonary spindle cell lesions in the setting of a uterine mass. **Key Words:** Solitary fibrous tumor—Uterus—Lung—Metastasis—Immunohistochemistry—Spindle cell—Malignant—STAT6.

Solitary fibrous tumor (SFT) is an uncommon mesenchymal neoplasm thought to be derived from fibroblast-like cells (1). SFTs can occur at virtually any anatomic location and can be exceptionally large at the time of presentation. In general, they are well-circumscribed lobulated tumors with a pale firm surface upon sectioning. The microscopic appearance of SFTs is often described as a "patternless" arrangement of bland, monomorphic spindle cells with areas of variable cellular density and is frequently characterized by the presence of branching, hemangiopericytoma (HPC)-like staghorn vessels. Histologically, the presence of increased mitotic figures (>4/10 high-power fields) and areas of tumor necrosis are defined as malignant (2). Whereas most are clinically benign, approximately 10%–15% of SFTs behave aggressively and may recur locally after resection or metastasize despite having a typical histologic appearance (3). For this reason, even SFTs with no overt features of malignancy are best regarded as tumors of uncertain malignant potential.

The pathologic diagnosis of SFT formerly relied on testing for CD34 expression by immunohistochemistry (IHC). However, it is now recognized that CD34

From the Division of Women's and Perinatal Pathology (K.C.S., M.R.N., B.E.H.); Department of Obstetrics and Gynecology, Division of Gynecologic Pathology, Brigham and Women's Hospital (K.M.E., M.G.M.); and Department of Medical Oncology, Dana-Farber Cancer Institute (S.C., S.G.), Boston, Massachusetts.

The authors declare no conflict of interest.

Address correspondence and reprint requests to Brooke E. Howitt, MD, Department of Pathology, Brigham and Women's Hospital, 75 Francis St., Amory 3, Boston, MA. E-mail: bhowitt@partners.org.

DOI: 10.1097/PGP.0000000000000197

is also expressed in multiple histologic mimics of SFT. Other markers, such as β-catenin and BCL-2, are similarly nonspecific. Recently, several studies using whole-exome and transcriptome sequencing have demonstrated that SFTs reliably contain a *NAB2-STAT6* gene fusion that results from a genomic inversion at the 12q13 locus (4–6). In the predicted fusion protein, the repressor domain of NGFI-A binding protein 2 (NAB2) is replaced by the carboxy-terminal portion of STAT6 (signal transducer and activator of transcription 6, interleukin-4 induced). The fusion protein is overexpressed in the nucleus, where it appears to act as a transcriptional activator of the EGR1 (early growth response 1) pathway. This discovery has translated into the use of STAT6 as a sensitive and specific IHC marker of SFT (7).

Although it was first described as a tumor of the pleura, primary SFT occurs more frequently at extrapleural sites (2). SFT of the female genital tract is extremely rare, with only a few cases of uterine SFT reported in the literature (8–10). In each of these cases, the patients were initially found to have a large uterine mass, and the diagnosis of SFT was established upon pathologic examination. Here, we describe the clinical course of a patient who presented with multiple lung nodules and a large uterine mass. The clinical scenario presented a diagnostic challenge because of the similar radiologic appearance of smooth muscle neoplasms such as leiomyosarcoma (LMS). The patient's diagnosis was firmly established only after pathologic analysis of both the primary tumor and a pulmonary nodule. To our knowledge, this is the first reported case of a uterine SFT presenting with pulmonary metastases.

MATERIALS AND METHODS

Clinical data were abstracted from the electronic medical record. Slides and paraffin blocks were obtained from the outside hospital where the fine-needle aspiration (FNA) of the lung mass was performed, and 4-μm-thick sections were cut from the cell block of the FNA material for IHC staining for STAT6. The hysterectomy resection specimen was fixed in 10% buffered formalin. Representative sections were embedded in paraffin, and 4-μm-thick sections were cut for hematoxylin and eosin staining and IHC studies. IHC for STAT6 was performed using a rabbit polyclonal antibody generated against the C-terminus of STAT6 (1:1000; sc-621; Santa Cruz Biotechnology, Santa Cruz, CA) using methods previously described (7).

RESULTS

Case History

An 81-yr-old woman with a past medical history of hypertension, hyperlipidemia, and uterine fibroids was referred to our institution for a second opinion regarding management of suspected metastatic uterine LMS. The patient had undergone a computed tomography (CT) scan of the chest for symptomatic shortness of breath that revealed a well-circumscribed nodule in the right upper lobe (RUL) of the lung measuring 0.8 cm (Fig. 1A). A repeat CT scan of the

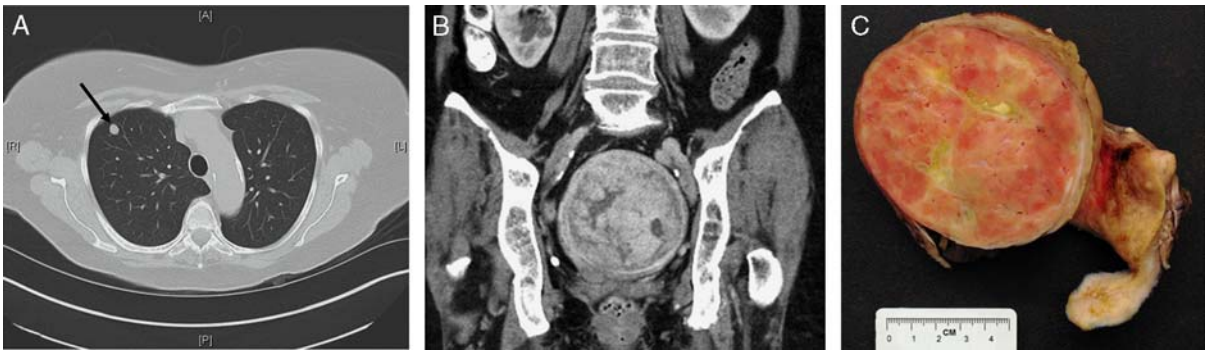

FIG. 1. Radiologic and gross images. (A) As part of an evaluation for long-standing shortness of breath, a chest CT demonstrated an 8 mm right upper lobe pulmonary nodule (arrow) and a 9 mm nodule in the left lower lobe. Follow-up CTs identified an additional right lower lobe nodule (3.5 mm) 3 mo after her initial presentation. (B) Biopsy of the pulmonary nodule was suspicious for an occult soft tissue malignancy, and follow-up abdominal CT revealed an 11 cm heterogenously enhancing uterine mass that was considered suspicious for leiomyosarcoma. (C) The 10 cm uterine mass was located in the myometrial wall. The well-circumscribed mass had a red-to-tan cut surface with foci of yellow degenerative change. CT indicates computed tomography.

chest 3 mo later demonstrated minimal growth of the RUL nodule but identified two additional nodules, one in the RUL (4 mm) and a second in the left lower lobe (LLL, 0.8×0.8 cm). Due to concern for metastatic disease, the patient underwent a diagnostic positron emission tomography-CT that demonstrated no fluorodeoxyglucose-avid lesions. A review of outside hospital imaging studies was notable for a uterine mass measuring 8.5×7.3 cm identified on a CT scan of the abdomen and pelvis (3.5 yr prior). This mass had grown from a 5.7 cm uterine mass initially identified on an ultrasound (6.5 yr prior), which was initially presumed to be a large uterine fibroid.

A CT-guided FNA of the larger RUL pulmonary nodule at an outside hospital revealed a spindle cell neoplasm concerning for metastasis from an occult soft tissue malignancy. A subsequent staging CT of the chest, abdomen, and pelvis revealed an increase in size and new heterogenous enhancement of the previously visualized dominant uterine mass ($11.1 \times 8.5 \times 8.2$ cm) (Fig. 1B). An interval increase was also observed in the LLL nodule from 0.8 to 1.1 cm, and an interval decrease was observed in the RUL nodule that was biopsied. An endometrial biopsy was attempted but was unsuccessful because of displacement of the cervix anteriorly beneath the pubic symphysis. The patient was given a presumptive diagnosis of metastatic LMS and was recommended to initiate chemotherapy with docetaxel and gemcitabine. Before initiating treatment, she sought a second opinion at our institution, where additional pathologic evaluation was performed on the biopsied lung nodule (see below), and it was recommended that the patient first undergo hysterectomy to confirm the diagnosis before initiating any medical therapy.

Microscopic Findings of the Lung Mass

The biopsy of the lung nodule revealed a tumor composed of spindle cells with minimal to mild nuclear pleomorphism and no necrosis or mitoses (Fig. 2A). IHC slides from the referring institution demonstrated tumor positivity for vimentin and BCL-2 and negative staining for S-100, cytokeratin, melan-A, actin, desmin, CD45, CD68, CD10, CD31, chromogranin, synaptophysin, ER, SOX-10, and c-kit. CD34 staining was equivocal, and Ki-67 was positive in approximately 10% of cells. IHC for STAT6 was performed at Brigham and Women's Hospital on the FNA cell block and demonstrated strong nuclear positivity in the lesional cells (Fig. 2B), supporting the diagnosis of SFT.

Gross and Microscopic Findings of the Uterine Mass

Gross examination of the resection specimen revealed a 482 g uterus with a large, well-circumscribed myometrial mass ($10.0 \times 10.0 \times 8.5$ cm) distorting the fundus of the uterus (Fig. 1C). The mass was predominantly mottled red-to-tan with central areas of yellow degenerative changes. The uterus also contained 2 submucosal leiomyomata (1.8 and 1.6 cm in greatest dimension) abutting the tumor. The mass was located less than a millimeter from the serosal surface and 0.2 cm from the endometrial surface, and there was no extension into the cervix. The serosal surface of the uterus was smooth and unremarkable. Histologically, the tumor was composed of relatively bland spindle cells with a patternless architecture and indistinct cell borders. The nuclei had dispersed chromatin and lacked nucleoli. There was marked variation in cellularity including areas of hyalinization, and the tumor contained well-developed branching, ectactic, HPC-like vessels (Fig. 2C). The neoplastic cells displayed low mitotic activity (1 mitotic figure per 10 high-power fields), and no obvious cytologic atypia, tumor necrosis, or dedifferentiation was present. IHC for STAT6 showed strong nuclear positivity (Fig. 2D). Additional IHC revealed CD34 positivity and no staining for SMA, desmin, or caldesmon. Cytogenetic analysis could not be performed because culture of the tumor cells was unsuccessful.

Clinical Follow-up

Because the patient was asymptomatic from her pulmonary metastatic disease, and given that medical therapy would be noncurative, the patient was observed after surgery. At 3- and 6-mo follow-up evaluations, the patient continued to be asymptomatic. A restaging CT scan 6 mo after hysterectomy demonstrated only a modest interval increase in the size of both the RUL pulmonary nodule (from 0.4×0.4 to 0.7×0.7 cm) and the LLL pulmonary nodule (1.2×1.0 to 1.3×1.1 cm). A third nodule in the RUL (0.4 cm) was unchanged.

DISCUSSION

All SFTs are considered to have malignant potential regardless of histologic appearance. In a study of 110 SFTs (2), risk factors for metastasis and

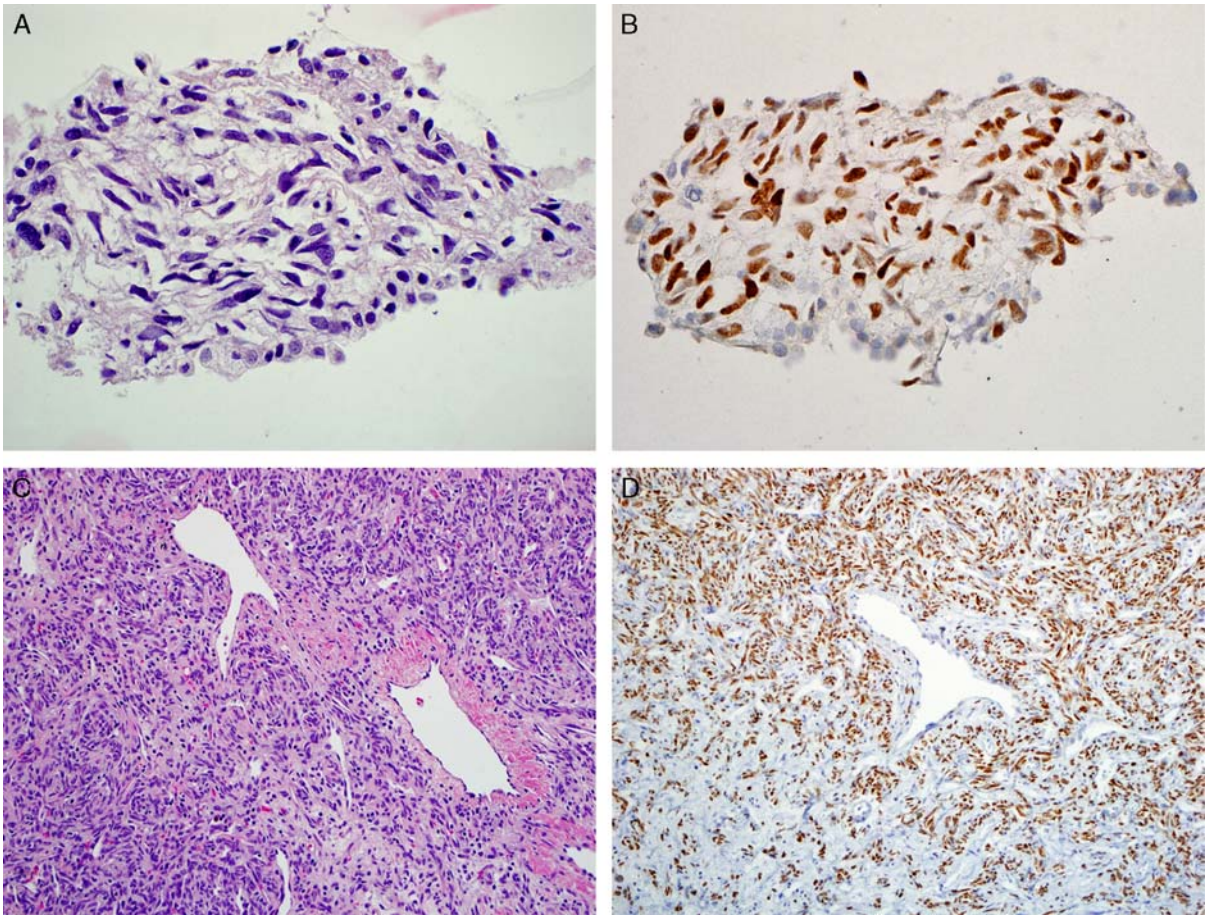

FIG. 2. Histologic appearance of pulmonary metastasis and uterine SFT. (A) H&E-stained cell block sections of the pulmonary metastasis showed a monomorphic spindle cell proliferation with mild nuclear pleomorphism. (B) Immunohistochemistry for STAT6 was diffusely and strongly positive in nuclei of the lesional cells. (C) H&E-stained sections of the uterine mass demonstrate a typical histologic appearance of solitary fibrous tumor, including bland spindle cells with a patternless architecture and branching ectatic staghorn vessels. (D) Immunohistochemistry for STAT6 on the uterine mass was diffusely and strongly positive in the nuclei of lesional cells, and the staining pattern highlights an area of variability in cellular density. H&E indicates hematoxylin and eosin.

mortality included advanced age at presentation, large tumor size, and increased mitoses, leading the authors to propose a 3-tiered model for risk stratification. The primary treatment of SFT is complete surgical excision. Adjuvant radiotherapy may help prevent local recurrence of histologically malignant tumors (11). There are no IHC or molecular markers that reliably distinguish clinically benign from malignant SFT.

The female genital tract is one of the rarest primary sites for SFT (12). Excluding the present case, we are aware of only 3 cases of uterine SFT reported in the literature (8–10), and this is the first documented case of a uterine SFT presenting with metastasis. When arising in the uterus, the diagnosis of SFT can be particularly challenging. Uterine SFT and benign leiomyomas present with similar symptoms and radiologic characteristics. A recent case report described a symptomatic SFT that was mistaken for a benign leiomyoma on the basis of preoperative imaging, and the diagnosis of SFT was made only after a therapeutic myomectomy (10). As exemplified in all of the case reports to date, the diagnosis of uterine SFT is seldom considered before pathologic evaluation; thus the pathologists' role is crucial for accurate diagnosis. A number of uterine tumors may share some histologic features with SFT, a subset of which may also metastasize to the lung. Therefore, the following discussion is based primarily on the differential diagnosis of a relatively bland spindle cell neoplasm in the uterus, which may also metastasize to the lung.

Uterine smooth muscle tumors are the most common mesenchymal neoplasms of the uterus. Leiomyomas

generally present as multiple masses of varying sizes, whereas LMS tends to present as a large, solitary or dominant mass. Histologically, LMS may have HPC-like vessels, but also demonstrate infiltration, cytologic atypia, high mitotic index, and geographic tumor necrosis. Uterine LMS frequently metastasize to the lung. Benign-appearing uterine smooth muscle tumors may rarely metastasize to the lung, a phenomenon known as benign metastasizing leiomyoma (BML). These unusual and somewhat controversial tumors occur primarily in women of reproductive age and contain a distinct cytogenetic profile (13). A definitive diagnosis of BML can be difficult to establish as it is essentially a diagnosis of exclusion requiring clinical correlation. Almost all smooth muscle tumors, including LMS and BML, are strongly positive for SMA, desmin, and caldesmon and negative for CD34 and STAT6.

Low-grade endometrial stromal neoplasia, like SFT, is characterized by relatively bland spindle cell morphology and a prominent vasculature. However, the vessels are rounded with thin muscular walls akin to arterioles, in contrast to the irregular, branching and very thin-walled vasculature of SFT. Endometrial stromal sarcoma may metastasize to the lung, in which case IHC may be helpful; CD10 is positive in low-grade endometrial stromal sarcoma, whereas CD34 and STAT6 are negative.

Another rare uterine neoplasm that shares some morphologic overlap with SFT and can metastasize to the lung is perivascular epithelioid cell tumor (PEComa). Malignant PEComas vary in their histologic appearance but typically have HPC-like vessels and are composed of plump epithelioid cells with abundant clear to eosinophilic cytoplasm with focally pleomorphic nuclei and prominent nucleoli, and may also exhibit a spindled component. PEComas typically stain for both melanocytic (HMB-45 and melan-A) and smooth muscle (SMA and desmin) markers by IHC (14), but are negative for CD34 and STAT6.

In summary, we have described the first known case of uterine SFT with metastasis to the lung at presentation. Given that other entities more commonly present in this manner (i.e. smooth muscle neoplasms), the diagnosis of metastatic uterine SFT was unexpected. Evaluation of STAT6 IHC at the primary and metastatic sites can be particularly useful in establishing the diagnosis. As illustrated by the case presented here, an accurate diagnosis is necessary to ensure appropriate clinical management. Moreover, the "benign" histology of this particular SFT underscores the need for additional pathologic or molecular criteria to identify the subset of SFT that will behave aggressively.

REFERENCES

1. Briselli M, Mark EJ, Dickersin GR. Solitary fibrous tumors of the pleura: eight new cases and review of 360 cases in the literature. *Cancer* 1981;47:2678–89.
2. Demicco EG, Park MS, Araujo DM, et al. Solitary fibrous tumor: a clinicopathological study of 110 cases and proposed risk assessment model. *Mod Pathol* 2012;25:1298–306.
3. Vallat-Decouvelaere AV, Dry SM, Fletcher CD. Atypical and malignant solitary fibrous tumors in extrathoracic locations: evidence of their comparability to intra-thoracic tumors. *Am J Surg Pathol* 1998;22:1501–11.
4. Mohajeri A, Tayebwa J, Collin A, et al. Comprehensive genetic analysis identifies a pathognomonic NAB2/STAT6 fusion gene, nonrandom secondary genomic imbalances, and a characteristic gene expression profile in solitary fibrous tumor. *Genes Chromosomes Cancer* 2013;52:873–86.
5. Robinson DR, Wu YM, Kalyana-Sundaram S, et al. Identification of recurrent NAB2-STAT6 gene fusions in solitary fibrous tumor by integrative sequencing. *Nat Genet* 2013;45:180–5.
6. Chmielecki J, Crago AM, Rosenberg M, et al. Whole-exome sequencing identifies a recurrent NAB2-STAT6 fusion in solitary fibrous tumors. *Nat Genet* 2013;45:131–2.
7. Doyle LA, Vivero M, Fletcher CD, et al. Nuclear expression of STAT6 distinguishes solitary fibrous tumor from histologic mimics. *Mod Pathol* 2014;27:390–5.
8. Wakami K, Tateyama H, Kawashima H, et al. Solitary fibrous tumor of the uterus producing high-molecular-weight insulin-like growth factor II and associated with hypoglycemia. *Int J Gynecol Pathol* 2005;24:79–84.
9. Chu PW, Liu JY, Peng YJ, et al. Solitary fibrous tumor of the uterus. *Taiwan J Obstet Gynecol* 2006;45:350–2.
10. Casanova J, Vizcaíno JR, Pinto F, et al. Abdominal mass mimicking a leiomyoma: Malignant uterine solitary fibrous tumor. *Gynecol Oncol Case Rep* 2012;2:143–5.
11. Gold JS, Antonescu CR, Hajdu C, et al. Clinicopathologic correlates of solitary fibrous tumors. *Cancer* 2002;94:1057–68.
12. Biedrzycki OJ, Singh N, Habeeb H, et al. Solitary fibrous tumor of the female genital tract a case report and review of the literature. *Int J Gynecol Pathol* 2007;26:259–64.
13. Nucci MR, Drapkin R, Dal Cin P, et al. Distinctive cytogenetic profile in benign metastasizing leiomyoma: pathogenetic implications. *Am J Surg Pathol* 2007;31:737–43.
14. Schoolmeester JK, Howitt BE, Hirsch MS, et al. Perivascular epithelioid cell neoplasm (PEComa) of the gynecologic tract: clinicopathologic and immunohistochemical characterization of 16 cases. *Am J Surg Pathol*. 2014 Feb;38(2):176–88.